Exploring Molecules beyond CO as Tip Functionalizations in High-Resolution Noncontact Atomic Force Microscopy

Xin, Xiaojun; Gan, Li Yong; VAN HOVE, M. A.; Ren, Xinguo; Wang, Hongyan; Guo, Chun Sheng; Zhao, Yong

Published in:
ACS Omega

DOI:
10.1021/acsomega.6b00168

Published: 30/11/2016

Document Version:
Publisher's PDF, also known as Version of record

ACS OMEGA

Article

http://pubs.acs.org/journal/acsodf

Exploring Molecules beyond CO as Tip Functionalizations in High-Resolution Noncontact Atomic Force Microscopy: A First Principles Approach

Xiaojun Xin,[†] Li-Yong Gan,[†] Michel A. Van Hove,[*,‡] Xinguo Ren,[§,∥] Hongyan Wang,[⊥] Chun-Sheng Guo,[*,†] and Yong Zhao[†]

[†]Key Laboratory of Advanced Technology of Materials (Ministry of Education), Superconductivity and New Energy R&D Center and [⊥]School of Physical Science and Technology, Southwest Jiaotong University, Chengdu 610031, Sichuan, China

[‡]Institute of Computational and Theoretical Studies and Department of Physics, Hong Kong Baptist University, Kowloon, Hong Kong Special Administrative Region

[§]Key Laboratory of Quantum Information and [∥]Synergistic Innovation Center of Quantum Information & Quantum Physics, University of Science and Technology of China, Hefei 230026, Anhui, China

ABSTRACT: Atomic resolution of molecules has been achieved using noncontact atomic force microscopy (AFM) with the key step to functionalize the tip apex by attaching suitable molecules so as to achieve high spatial resolution through a sharper tip. A few molecular terminations have been explored theoretically and experimentally, and they exhibit various imaging behaviors. Here, we explore the influence of the structures and chemical compositions of various molecular candidates as tips on the contrast of AFM images by a first principles approach. Our results reveal that the two end atoms of a linear molecule terminating nearest the sample dominate the imaging behaviors, for example, atomic resolution, sharpness, distortion, and so forth, whereas the symmetry of the termination plays an important role in the distortion of AFM images. These findings suggest that new tip terminations can be engineered by decoupling the three end atoms responsible for imaging behaviors from the tip structure behind them, which is attached to the macro tip apex.

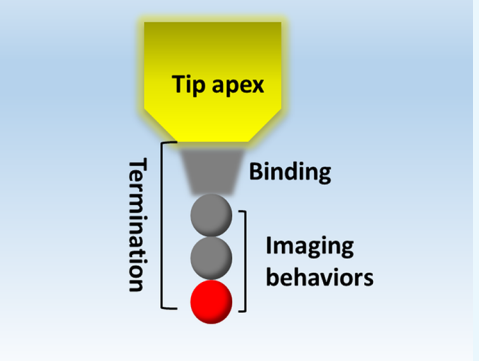

1. INTRODUCTION

In scanning probe microscopy, it is commonly known that the structure and atomic compositions of the tip apex have a significant influence on the spatial resolution of the image. Particularly, CO functionalization is a key step for noncontact atomic force microscopy (AFM) to achieve remarkable atomic resolution for planar molecules.[1] This technique has achieved great progress in the past few years.[2−11] For example, it has been reported that carbon−carbon bond orders within polycyclic aromatic hydrocarbons and fullerenes can be distinguished.[11] The intricate chemical transformation of an individual molecule[7] and even its subatomic resolution[2,12,13] have been directly imaged.

Recently, numerous studies have paid attention to how a tip affects the image contrast in AFM measurements. For example, it was proposed that the sharp resolution originates from the ridge between two minima of the surface potential imaged by the flexible probe.[14,15] It has been found that the metallic tip behind CO gives a minor contribution to the AFM resolution,[16] whereas the next-to-last atom is important for the AFM imaging. For example, O_2, Cu_3CuO, and CO tips present very different imaging behaviors,[1,17] where the metal−O tip produces a blurry image compared with that of the CO tip, whereas the theoretical image of an O_2 tip yields an image in which it is difficult to interpret the atomic skeleton. On the other hand, a CH_4 termination produces a simulated AFM image,[16] which is similar to the experimental result obtained by a pentacene tip with −CH termination,[1] and an O-down-oriented naphthalene tetracarboxylic diimide (NTCDI) tip can perform well in AFM imaging.[18] More recently, the imaging behaviors of Br, Xe, Kr, and NO terminations for AFM imaging have been examined experimentally, and it was found that the Br tip is particularly useful because it is much easier to prepare and well-suited for the lateral manipulation of single molecules.[19] These studies suggest that exploring various molecular terminations is valuable.

In this study, we systematically examine the imaging behaviors of various molecular candidates as tips on the AFM contrast with a first principles approach. For a linear molecule pointing perpendicularly toward the sample surface, only the two end atoms are found to dominate the ability for atomic resolution; in particular, CO_2 and SCO tips can perform as well

Received: August 2, 2016
Accepted: November 9, 2016
Published: November 21, 2016

DOI: 10.1021/acsomega.6b00168
ACS Omega 2016, 1, 1004−1009

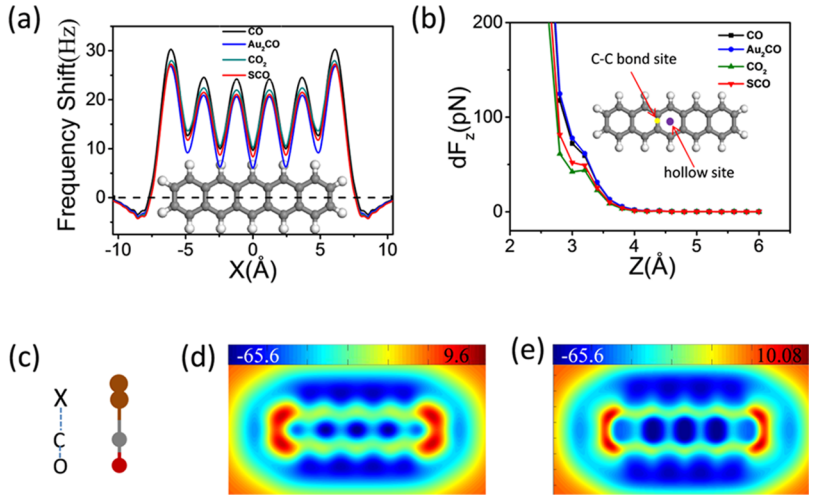

Figure 1. (a) FS line profiles of a pentacene molecule along its long axis obtained with CO (black), Au_2CO (blue), CO_2 (green), and SCO (red) terminations. (b) Difference $dF_Z = F_Z^{bond} - F_Z^{hollow}$ between the interaction forces at the C−C bond site and the hollow site (marked by arrows) as a function of the scanning height Z for the four terminations. (c) Schematic illustration of X−CO tip terminations, where X can be Au_2, S, O, and so forth denoted by two brown balls and the end atoms C and O are denoted by gray and red balls, respectively. (d) and (e) 2D force patterns (red/blue = large/small repulsive force) obtained with a CO_2 termination, without and with accounting for the tilting effect of the tip.

as a CO tip. With an asymmetric molecule termination, for example, a planar H_2CO with CO pointing toward the sample, dramatically distorted images are yielded depending on the H···H orientations, indicating that the symmetry of the molecular terminations plays an important role in the distortion of AFM images.

2. METHODOLOGY

Our simulations are based on a model we built that can well reproduce the AFM images:[20] it employs the Fritz Haber Institute ab initio molecular simulations code package[21] with an accurate atomic-centered basis set and grid-based real-space integration of "*tight*" settings. The density functional theory (DFT) + vdW method of Tkatchenko and Scheffler[22] is applied to account for the van der Waals interactions. The generalized gradient approximation of Perdew, Burke, and Ernzerhof[23] is chosen for the exchange−correlation functional used in the DFT calculations. The frequency shift (FS) profiles are calculated by differentiating the corresponding interaction force according to $\Delta f(x, y, z) = -\frac{f_0}{2k_0}\frac{\partial F_z(x,y,z')}{\partial z'}\Big|_{z'=z}$, where f_0 and k_0 are the resonance frequency and the spring constant of the macroscopic tip, respectively.[24]

In our simulations, the substrate is not included because it yields a nearly uniform background for various tip terminations. The tips are oriented perpendicularly to the main plane of the planar sample molecules, whereas in most of our calculations, the tip molecule is allowed to tilt under the influence of lateral AFM forces. Because the tip is flexible, we include a lateral spring constant k of the tip of 0.5 N/m when appropriate.[20] Indeed, the lateral stiffness of different tips is quite different, whereas the lateral spring constant is unknown, and there are no corresponding experimental images. In this study, we mainly discuss the difference in images obtained with rigid tips. The two-dimensional (2D) maps are calculated by moving the tip over the sample molecule on a lateral grid of x and y positions with intervals of 0.2 Å in both directions.

3. RESULTS AND DISCUSSION

3.1. CO as the First Two End Atoms. We first study linear molecules/structures at the tip terminations. We take pentacene as the benchmark sample molecule to be imaged because it has been extensively studied in previous AFM studies.[1,3,16] With tips of aligned Au_2CO and linear molecules CO_2 and SCO, FS line profiles along the long axis of the pentacene molecule obtained with these tips are shown in Figure 1a. Clearly, each of these tips yields five FS minima over the hollow sites of the pentacene and two FS minima at both ends corresponding to the halo observed around the sample molecule[1] (similar to the blue halo around the molecule, which can be seen in Figure 1d or 1e). Specifically, removing the metallic part Au_2 from the Au_2CO tip is seen to have little effect on the atomic-scale FS corrugation. This is understandable because the Au_2 yields only an attractive background because of its relatively distant location far from the sample (distance larger than 5 Å) and also because it weakly affects only the electronic state of CO. More remarkably, FS profiles by CO_2 and SCO molecules are also very close to that of Au_2CO. The four tip terminations share a great similarity of the corrugation over pentacene at the same scanning height, whereas the electronic structure of the CO molecule, as is known, is remarkably different from the −CO group bonding to the third atom, for example, O in CO_2 or S in SCO.

To further investigate the influence of tip compositions behind the two end atoms at various scanning heights, we introduce the interaction force difference (dF_Z) at different positions, for example, $dF_Z = F_Z^{bond} - F_Z^{hollow}$, which is the difference between the forces at the C−C bond of pentacene and at the hollow site obtained by CO, Au_2CO, CO_2, and SCO tips, shown in Figure 1b. This difference in force not only highlights the corrugation near the central C_6 ring of pentacene observed with a specific tip termination but also can be used to compare the corrugation evolution with different terminations at increasing scanning height. As shown in Figure 1b, in general, the CO_2 tip yields the smallest corrugation, and Au_2CO and CO yield the largest at the same scanning height. They all measure larger repulsive forces at the C−C bond ($dF_Z > 0$),

DOI: 10.1021/acsomega.6b00168
ACS Omega 2016, 1, 1004−1009

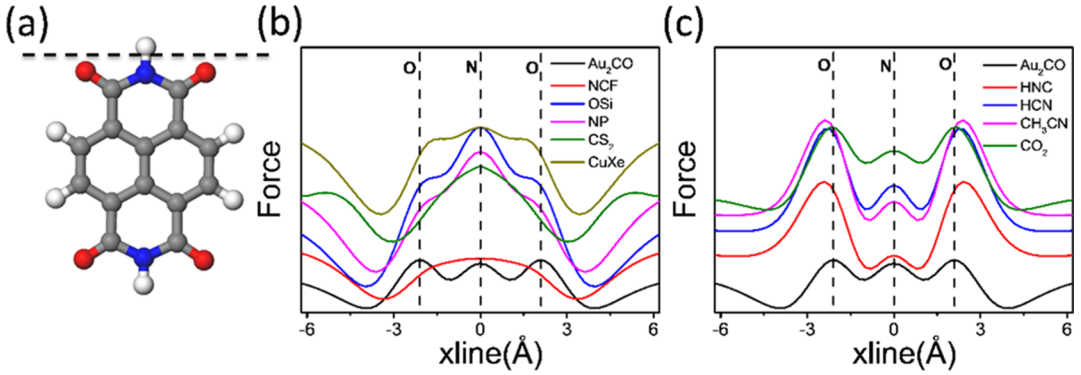

Figure 2. (a) Chemical structure of NTCDI, where C, H, O, and N atoms are shown in gray, white, red, and blue, respectively. (b) and (c) Force line profiles along the black dashed line marked in (a) over the O and N atoms with different tips at their appropriate scan heights. For clarity, forces of different tips in (b) and (c) are added with different values to separate the lines.

indicating that the same contrast is imaged by various X−CO tips at a given scanning height. When the scanning height is larger than 3.8 Å, dF_Z for the four tips decreases to zero and the contrast corrugation vanishes. The dependence of the AFM contrast on the scanning height of these tips agrees well with that of CO tip, which has been experimentally and theoretically discussed in previous studies.[1,16] In the following, we will simply discuss the images obtained at a constant scanning height.

For a more global view, we show in Figure 1d,e the 2D force patterns obtained with a CO_2 termination, without and with accounting for the tilting effect of the tip due to the lateral AFM forces. Images for CO, Au_2CO, and SCO tips are not shown because they are nearly identical to those for CO_2 tips, not only for atomic resolution but also for distortions. Clearly, the CO_2 termination can image well the chemical structure of pentacene. By introducing the tilting effect, the hexagonal C_6 rings appear stretched considerably along the short axis, closely consistent with the image obtained with CO termination experimentally and theoretically.[1,20] All of these findings suggest that compositions behind the two end atoms of a linear termination have little influence on the imaging behaviors, even if the electronic structures of the two end atoms are modified.

3.2. Effect of the First End Atom. For a comprehensive exploration of the structures and chemical compositions of the linear tip terminations on the AFM contrast, we test various tip candidates for their imaging capability over NTCDI (shown in Figure 2a), which includes O and N elements in addition to C and H. The end atom of a tip termination can be C, N, O, F, Si, P, S, Cl (not shown, identical to F), and Xe, and the second and third (if present) end atoms are carefully chosen to be linear molecules/groups. Generally speaking, most tips can image the skeleton of the hexagonal C_6 rings well, for example, the central two C_6 rings of NTCDI, because of their simple ring structure. Nevertheless, the global contrast over NTCDI obtained with these tips varies a lot. For a clear view, we show in Figure 2b,c the force line profiles along the dashed black line marked in Figure 2a over the N and O atoms. The peaks of the line profiles at atom positions can be used to evaluate the capability of a tip to distinguish N and O atoms. Compared with the benchmark of Au_2CO tip, which shows three peaks of N and two peaks of O atoms, Xe shows only a sharp peak at the N position, as shown in Figure 2b, although it enhanced the contrast of scanning tunneling microscopy[19] and yields blurred but less distorted images of other polycyclic aromatic hydrocarbons. For F, Si, P, S, and Cl (not shown) atoms as the first end atom, similar to the Xe case, there arises only one peak over the N atoms with shoulders over the O atoms, suggesting that atomic resolution is not achieved. Here, the role of the second end atom is not discussed because we cannot consider all of the pairing possibilities. Because it is the two end atoms that dominate the AFM contrast, we do not rule out the possibility that some molecules terminated with F, Si, P, S, or Cl as the first end atom may be able to produce good AFM images.

By contrast, with C, N, or O as the first end atom, force line profiles shown in Figure 2c suggest that HNC, HCN, CH_3CN (linear three end atoms), and CO_2 terminations can perform as well as the Au_2CO tip. They yield three peaks over the N position and two peaks over the O position, indicating the apparent identification of O and N atoms, although the brightness of the N atom is slightly weaker than that of O atoms. Impressively, a CH_3CN tip can perform as well as HCN, which not only confirms that the two end atoms dominate the capability for AFM imaging but also suggests that the chemical compositions behind the two end atoms can be carefully chosen for attaching the metallic tip. This facilitates the design of practically useful tip functionalizations for AFM.

3.3. Imaging Behaviors of −CN Tips. Considering that few molecules are terminated by a C atom and −CO tips have been widely studied, in the following, we focus on tips with −CN as the two end atoms. For simplicity, linear HCN and ClCN with H and more electronegative Cl as the third end atom are chosen, pointing perpendicularly to the sample surface. The 2D patterns of a pentacene sample obtained with HCN and ClCN are shown in Figure 3c,d in comparison with that obtained by CO_2 in Figure 3b. X−CN (X = H, Cl) tips exhibit well the skeleton of the pentacene molecule, showing clearly the five hollows, two brighter ends, and, to a lesser degree, the C−H bonds.[1,20] Moreover, it is interesting that the pattern obtained with X−CN seems to be less distorted than that obtained with X−CO. Comparing the images in Figure 3b−d, which allow tip tilting by including a lateral spring constant of 0.5 N/m, the central three hollows obtained with ClCN are apparently less stretched along the short pentacene axis. For the well-known chemical geometry of pentacene, the apparent increase obtained with CO_2 in the C−C bond lengths is up to 70% from free pentacene, nearly identical to the distortion found with CO tips,[3,20] whereas that obtained with HCN and ClCN is only around 45%.

To investigate the imaging behaviors of the X−CN tips in more detail, we use the sample molecule 4-(4-(2,3,4,5,6-

DOI: 10.1021/acsomega.6b00168
ACS Omega 2016, 1, 1004−1009

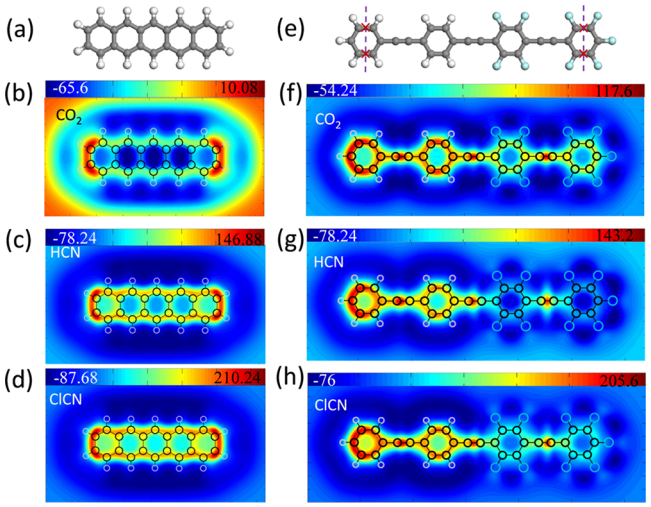

Figure 3. Chemical structure of pentacene (a) and FFPB molecules (e) where C, H, and F are denoted by gray, white, and light blue balls, respectively. The red crosses denote positions of the C−C bonds used to measure their mutual distance across the rings. Force maps (red/blue = large/small repulsive force) of the pentacene and FFPB molecules obtained with flexible CO_2 (b) and (f), HCN (c) and (g), and ClCN (d) and (h), at a tip height of 3.2 Å. Atom positions are marked by circles in the 2D patterns.

pentafluorophenylethynyl)-2,3,5,6-tetrafluorophenylethynyl) phenylethynylbenzene (FFPB),[3,25] which has been used to discuss the image distortions by CO termination reported by Moll et al.[26] FFPB has four phenyl rings connected by ethynylene units (C≡C triple bonds), two of these phenyl rings being H-terminated (H-ring) and the other two being F-terminated (F-ring), as shown in Figure 3e. We show in Figure 3f−h the 2D patterns obtained with CO_2, HCN, and ClCN terminations, including the tilting effect at 3.2 Å scanning height. Clearly, the three simulated images share great similarity: the C≡C triple bonds are imaged as bright lines perpendicular to the bond, and C−F can be resolved well, whereas C−H cannot be resolved, which is in good agreement with the experimental result obtained with CO termination. Because of the FFPB molecule being free in our simulation, the H-rings and F-rings exhibit different magnitudes of brightness, which is not so obvious in the image of the experiment.[26] We measure the image distortion as the distance between the two apparent C−C bond positions denoted with red crosses in Figure 3e: this distortion is given in Table 1 for different tip terminations. In our simulation, the H-rings appear larger in diameter than the F-rings, using a CO_2 tip, which is consistent with the report by Moll et al., using the CO tip.[26] The HCN and ClCN tips also yield larger apparent H-rings than F-rings. Compared with the well-known 2.42 Å distance between the midpoints of opposite C−C bonds in phenyl rings, the H-ring is enlarged/contracted by 6 and −2% with rigid X−CO (X = none or O) versus X−CN (X = H or Cl), respectively, and by −9 and −15% for the F-ring It appears that the X−CN tips indeed image the polycyclic aromatic hydrocarbons (carbon rings with H-terminations) with less distortion than the X−CO tips.

Table 1. Geometric Distance and Apparent Distance from the Computed FS with Rigid CO, HCN, and ClCN between the Two C−C Bonds of FFPB Molecules Marked by Red Crosses in Figure 3e

	geometry	CO	HCN	ClCN
H-ring (Å)	2.42	2.54	2.38	2.38
F-ring (Å)	2.42	2.20	2.06	2.06

3.4. Effect of the Molecule Symmetry. So far we have discussed linear molecules (including CH_3CN with three linear end atoms) as the AFM tip terminations, whereas most molecular candidates are not linear. The two end atoms are indeed crucial for the AFM imaging, whereas the symmetry of the tip molecule (referencing to the sample) is also important, specifically for the distortion of the AFM images. Here, we choose a planar H_2CO molecule, with CO as the two end atoms pointing toward the sample and two H atoms able to be in different orientations, either parallel to the long axis of pentacene (αH_2CO) or perpendicular to it (βH_2CO), as sketched in Figure 4a,b. The 2D patterns of pentacene obtained by αH_2CO and βH_2CO tips are shown in Figure 4c,d. Apparently, while the chemical structures of the five C_6 rings are imaged, a remarkable difference in distortion arises: patterns of the hollows obtained by αH_2CO look stretched along the long axis, whereas those for βH_2CO are stretched along the short axis. The dramatic visual impression comes mostly from the shapes of the hollows (minimum areas), which are differently distorted by αH_2CO and βH_2CO tips, whereas the apparent lengths of pentacene (distance between the first and sixth C−C bonds) by αH_2CO is only 3% larger. Distortion due to the orientations of the H···H in H_2CO is much more remarkable for the NTCDI sample, as shown in Figure 4e,f, which are obtained with αH_2CO and βH_2CO for H···H parallel and perpendicular to the N···N in NTCDI, respectively. Generally speaking, the image is stretched along/perpendicular to the N···N orientation of NTCDI by $\alpha H_2CO/\beta H_2CO$. The

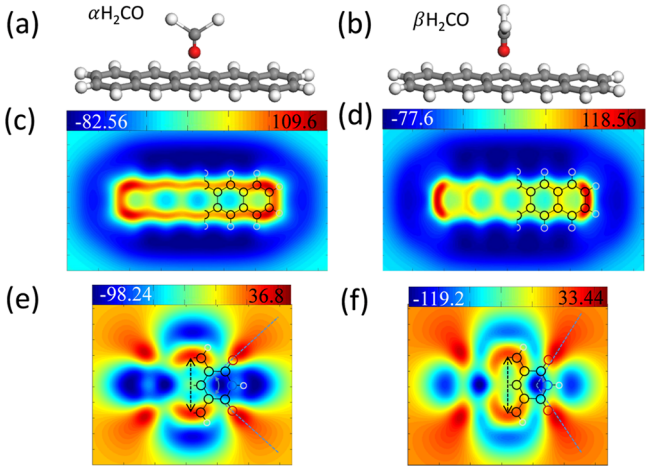

Figure 4. (a) and (b) Models of H_2CO with its H···H pair parallel to (αH_2CO) or perpendicular to (βH_2CO) the long axis of the pentacene molecule. 2D force patterns (red/blue = large/small repulsive force) of the pentacene molecule obtained with αH_2CO (c) and βH_2CO (d). (e) and (f) 2D patterns of the molecule obtained by H_2CO with its H···H pair parallel to (αH_2CO) or perpendicular to (βH_2CO) the N···N pair in NTCDI. The dashed double-headed arrows denote the apparent distance of C−C bonds and the blue dashed lines mark the angle between the two apparent CO bonds. For clarity, only half of the atom positions are marked by circles in the 2D patterns. Panels (c) and (d) use the same length scale, which is different from panels (a) and (b).

DOI: 10.1021/acsomega.6b00168
ACS Omega 2016, 1, 1004−1009

apparent distance between the two C−C bonds (marked by dashed arrows in Figure 4,d) imaged by αH_2CO is 3% smaller than the chemical structure (4.87 vs 4.72 Å), whereas that imaged by βH_2CO is around 3% larger; the angle between the two apparent C−O bonds (marked by the dashed angles) by αH_2CO is 30% smaller than the chemical structure (82° vs 116.4°), whereas that by βH_2CO is around 120°.

In our simulations, distortions due to the symmetry of the molecule terminations are always observed, which are mainly affected by the third atoms (e.g., two H atoms in H_2CO) behind the linear two end atoms, whereas the influence of the fourth atoms (e.g., the three H atoms in CH_3CO) is small. Taking the third atoms as a group in a plane parallel to the sample, generally images are stretched along its long axis, whereas they are compressed along its short axis. Nevertheless, the symmetry of the metallic tip, for example, Cu clusters, behind CO hardly affects the distortion. Using a cluster with three aligned Cu atoms as the third atoms parallel to the sample and CO adsorbed at the middle Cu as the two end atoms pointing to the sample, we find that different orientations of the three aligned Cu atoms referenced to the sample induce little distortion of the image compared with that obtained by an isolated CO tip. In this case, the electronic structure of the end atoms does not change much, and the metallic part only provides a weak asymmetric background.

4. CONCLUSIONS

In conclusion, we have systematically explored the AFM contrast produced by various molecular candidates as AFM terminations. C, N, and O as the first end atoms produce sharper images for adjacent atoms than Si, P, and S, which suggests that atomic sizes are of great influence on the capability for atomic resolutions. The second period light element atoms as the first end atom in the inert molecule tips could be favorable for high resolution AFM imaging. With linear molecules, only the two end atoms are found to dominate the imaging behaviors for AFM imaging: in particular, SCO and CO_2 can perform equally to a CO termination, and the images obtained with HCN, ClCN, and CH_3CN are nearly identical; however, the tips of NCF, CS_2, and NP are found with difficulty to distinguish adjacent atoms. Distortion of the image depends slightly on the atoms behind the first two, whereas it varies a lot depending on the symmetry of the tip termination. These findings suggest that new tip terminations can be engineered by decoupling the three end atoms responsible for imaging from the tip structure behind them, which is attached to the macro tip apex.

AUTHOR INFORMATION

Corresponding Authors

*E-mail: vanhove@hkbu.edu.hk (M.A.V.H.).
*E-mail: csguo@swjtu.edu.cn (C.-S.G.).

ORCID

Michel A. Van Hove: 0000-0002-8898-6921

Notes

The authors declare no competing financial interest.

ACKNOWLEDGMENTS

This work was supported by the Natural Science Foundation of China (no. 51302231 and no. 11374276), by the Fundamental Research Funds for the Central Universities (SWJTU2682013RC02, SWJTU11ZT31, and SWJTU2682016ZDPY10), and in part by the Research Grants Council of HKSAR (project no. 9041650). M.A.V.H. was supported by the HKBU Strategic Development Fund.

REFERENCES

(1) Gross, L.; Mohn, F.; Moll, N.; Liljeroth, P.; Meyer, G. The Chemical Structure of a Molecule Resolved by Atomic Force Microscopy. *Science* **2009**, *325*, 1110−1114.

(2) Emmrich, M.; Huber, F.; Pielmeier, F.; Welker, J.; Hofmann, T.; Schneiderbauer, M.; Meuer, D.; Polesya, S.; Mankovsky, S.; Kodderitzsch, D.; Ebert, H.; Giessibl, F. J. Subatomic resolution force microscopy reveals internal structure and adsorption sites of small iron clusters. *Science* **2015**, *348*, 308−311.

(3) Neu, M.; Moll, N.; Gross, L.; Meyer, G.; Giessibl, F. J.; Repp, J. Image correction for atomic force microscopy images with functionalized tips. *Phys. Rev. B: Condens. Matter Mater. Phys.* **2014**, *89*, 205407.

(4) Boneschanscher, M. P.; Hämäläinen, S. K.; Liljeroth, P.; Swart, I. Sample Corrugation Affects the Apparent Bond Lengths in Atomic Force Microscopy. *ACS Nano* **2014**, *8*, 3006−3014.

(5) Zhang, J.; Chen, P.; Yuan, B.; Ji, W.; Cheng, Z.; Qiu, X. Real-Space Identification of Intermolecular Bonding with Atomic Force Microscopy. *Science* **2013**, *342*, 611−614.

(6) Schuler, B.; Liu, W.; Tkatchenko, A.; Moll, N.; Meyer, G.; Mistry, A.; Fox, D.; Gross, L. Adsorption Geometry Determination of Single Molecules by Atomic Force Microscopy. *Phys. Rev. Lett.* **2013**, *111*, 106103.

(7) de Oteyza, D. G.; Gorman, P.; Chen, Y.-C.; Wickenburg, S.; Riss, A.; Mowbray, D. J.; Etkin, G.; Pedramrazi, Z.; Tsai, H.-Z.; Rubio, A.; Crommie, M. F.; Fischer, F. R. Direct Imaging of Covalent Bond Structure in Single-Molecule Chemical Reactions. *Science* **2013**, *340*, 1434−1437.

(8) Pavliček, N.; Fleury, B.; Neu, M.; Niedenführ, J.; Herranz-Lancho, C.; Ruben, M.; Repp, J. Atomic Force Microscopy Reveals Bistable Configurations of Dibenzo[*a*,*h*]thianthrene and Their Interconversion Pathway. *Phys. Rev. Lett.* **2012**, *108*, 086101.

(9) Guillermet, O.; Gauthier, S.; Joachim, C.; de Mendoza, P.; Lauterbach, T.; Echavarren, A. STM and AFM high resolution intramolecular imaging of a single decastarphene molecule. *Chem. Phys. Lett.* **2011**, *511*, 482−485.

(10) Moll, N.; Gross, L.; Mohn, F.; Curioni, A.; Meyer, G. The mechanisms underlying the enhanced resolution of atomic force microscopy with functionalized tips. *New J. Phys.* **2010**, *12*, 125020.

(11) Gross, L.; Mohn, F.; Moll, N.; Schuler, B.; Criado, A.; Guitian, E.; Pena, D.; Gourdon, A.; Meyer, G. Bond-Order Discrimination by Atomic Force Microscopy. *Science* **2012**, *337*, 1326−1329.

(12) Hofmann, T.; Pielmeier, F.; Giessibl, F. J. Chemical and crystallographic characterization of the tip apex in scanning probe microscopy. *Phys. Rev. Lett.* **2014**, *112*, 066101.

(13) Welker, J.; Weymouth, A. J.; Giessibl, F. J. The influence of chemical bonding configuration on atomic identification by force spectroscopy. *ACS Nano* **2013**, *7*, 7377−7382.

(14) Hapala, P.; Kichin, G.; Wagner, C.; Tautz, F. S.; Temirov, R.; Jelínek, P. Mechanism of high-resolution STM/AFM imaging with functionalized tips. *Phys. Rev. B* **2014**, *90*, 085421.

(15) Hapala, P.; Temirov, R.; Tautz, F. S.; Jelínek, P. Origin of High-Resolution IETS-STM Images of Organic Molecules with Functionalized Tips. *Phys. Rev. Lett.* **2014**, *113*, 226101.

(16) Guo, C.-S.; Van Hove, M. A.; Zhang, R.-Q.; Minot, C. Prospects for Resolving Chemical Structure by Atomic Force Microscopy: A First-Principles Study. *Langmuir* **2010**, *26*, 16271−16277.

(17) Mönig, H.; Hermoso, D. R.; Arado, O. D.; Todorović, M.; Timmer, A.; Schüer, S.; Langewisch, G.; Pérez, R.; Fuchs, H. Submolecular Imaging by Noncontact Atomic Force Microscopy with an Oxygen Atom Rigidly Connected to a Metallic Probe. *ACS Nano* **2016**, *10*, 1201−1209.

(18) Sweetman, A. M.; Jarvis, S. P.; Sang, H.; Lekkas, I.; Rahe, P.; Wang, Y.; Wang, J.; Champness, N. R.; Kantorovich, L.; Moriarty, P.

DOI: 10.1021/acsomega.6b00168
ACS Omega 2016, 1, 1004−1009

Mapping the force field of a hydrogen-bonded assembly. *Nat. Commun.* **2014**, *5*, 3931.
(19) Mohn, F.; Schuler, B.; Gross, L.; Meyer, G. Different tips for high-resolution atomic force microscopy and scanning tunneling microscopy of single molecules. *Appl. Phys. Lett.* **2013**, *102*, 073109.
(20) Guo, C.-S.; Van Hove, M. A.; Ren, X.; Zhao, Y. High-Resolution Model for Noncontact Atomic Force Microscopy with a Flexible Molecule on the Tip Apex. *J. Phys. Chem. C* **2015**, *119*, 1483−1488.
(21) Blum, V.; Gehrke, R.; Hanke, F.; Havu, P.; Havu, V.; Ren, X. G.; Reuter, K.; Scheffler, M. Ab initio molecular simulations with numeric atom-centered orbitals. *Comput. Phys. Commun.* **2009**, *180*, 2175−2196.
(22) Tkatchenko, A.; Scheffler, M. Accurate Molecular van der Waals Interactions from Ground-State Electron Density and Free-Atom Reference Data. *Phys. Rev. Lett.* **2009**, *102*, 073005.
(23) Perdew, J. P.; Burke, K.; Ernzerhof, M. Generalized gradient approximation made simple. *Phys. Rev. Lett.* **1996**, *77*, 3865−3868.
(24) Sader, J. E.; Jarvis, S. P. Accurate formulas for interaction force and energy in frequency modulation force spectroscopy. *Appl. Phys. Lett.* **2004**, *84*, 1801−1803.
(25) Matsuo, D.; Yang, X.; Hamada, A.; Morimoto, K.; Kato, T.; Yahiro, M.; Adachi, C.; Orita, A.; Otera, J. Fluoro-substituted Phenyleneethynylenes: Acetylenic n-Type Organic Semiconductors. *Chem. Lett.* **2010**, *39*, 1300−1302.
(26) Moll, N.; Schuler, B.; Kawai, S.; Xu, F.; Peng, L.; Orita, A.; Otera, J.; Curioni, A.; Neu, M.; Repp, J.; Meyer, G.; Gross, L. Image Distortions of a Partially Fluorinated Hydrocarbon Molecule in Atomic Force Microscopy with Carbon Monoxide Terminated Tips. *Nano Lett.* **2014**, *14*, 6127−6131.

DOI: 10.1021/acsomega.6b00168
ACS Omega 2016, 1, 1004−1009